

Electronic Supplementary Information

A polar oxyhalogen-vanadate compound (C₅NH₁₃Cl)₂VOCl₄ with optical and two-staged dielectric switch behavior

Qing-Rong Kong, Bin Wang, Xiao-Lin Liu, Hai-Xia Zhao, La-Sheng Long* and Lan-Sun Zheng*

Collaborative Innovation Center of Chemistry for Energy Materials, State Key Laboratory of Physical Chemistry of Solid Surfaces and Department of Chemistry, College of Chemistry and Chemical Engineering, Xiamen University, Xiamen 361005, P. R. China.

*Corresponding author.

E-mail address: lslong@xmu.edu.cn; hxzhao@xmu.edu.cn.

Single-Crystal Structure Determination. Variable-temperature X-ray single diffraction data were collected by an Agilent Supernova CCD diffractometer in a ω -scan mode with $\Delta\omega = 1.0^\circ$. The structure data were collected at 200 K, 300 K and 365 K respectively by using a Cu-K α ($\lambda = 1.5418 \text{ \AA}$) radiation. Data collection and processing were performed by CrysAlis PRO program. The structures were solved by direct methods (ShelXT),^{S1} and nonhydrogen atoms were refined by full-matrix methods based on F^2 by means of ShelXL on the OLEX2 program.^{S2, S3} All H atoms were refined using a riding model. CCDC 2055429 (LTP-200 K), 2055430 (ITP-300 K) contain the supplementary crystallographic data for this paper. These data can be obtained free of charge from the Cambridge Crystallographic Data Centre.

Variable-Temperature Powder X-ray Diffraction. Variable temperature Powder X-ray Diffraction (PXRD) patterns were collected by a Bruker D8 Discover X-ray Powder Diffractometer in helium atmosphere at 300 K (ITP) and 400 K (HTP)(Fig.

S1).

Thermal Properties. Thermogravimetric analysis (TGA) was performed using an SDT-Q600 thermal analyzer in nitrogen atmosphere at a heating rate of $10 \text{ K}\cdot\text{min}^{-1}$ (Fig. S5). Differential scanning calorimetry (DSC) measurements were collected using a NETZSCH DSC 200F3 instrument with heating and cooling rates of $10 \text{ K}\cdot\text{min}^{-1}$ under nitrogen atmospheres (Fig. 3).

Dielectric Measurements. The temperature-dependent dielectric permittivity ε ($\varepsilon = \varepsilon' - i\varepsilon''$) was measured using the two-probe *a.c.* impedance method in the testing temperature range from 100 to 400 K and the frequency range from 100 Hz to 1 MHz on Wayne Kerr 6500B analyzer.

Optical Second Harmonic Generation (SHG). SHG activities were recorded using powder sample with sizes of 80-100 μm . An unexpanded laser (OPOTEK, 355 II) with a low divergence (Nd: YAG, 1064 nm, 5 ns, 10 Hz repetition rate, 1.6 MW peak power) was used.

Caution! The high-power laser is dangerous for the eyes; adequate eye protection is necessary during the SHG experiments.

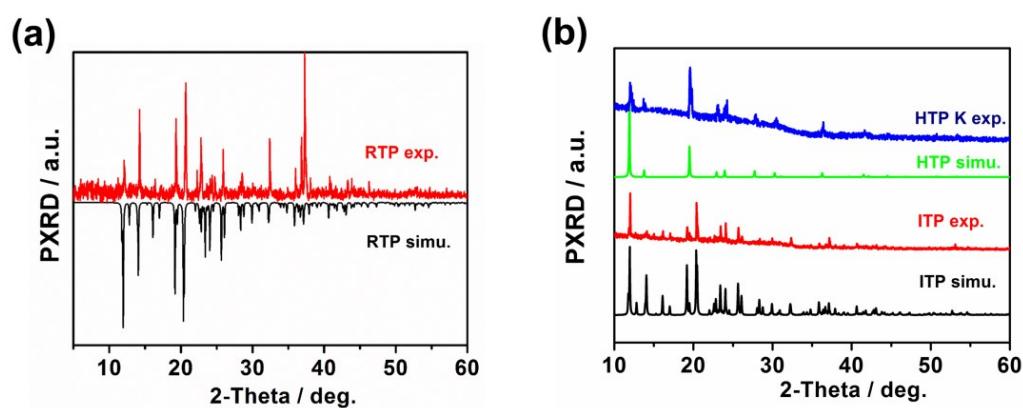


Fig. S1. (a) Simulated and experimental PXRD powder patterns for **1** at room temperature. (b) Variable temperature PXRD patterns at 300 K (ITP) and 400 K (HTP) for **1**.

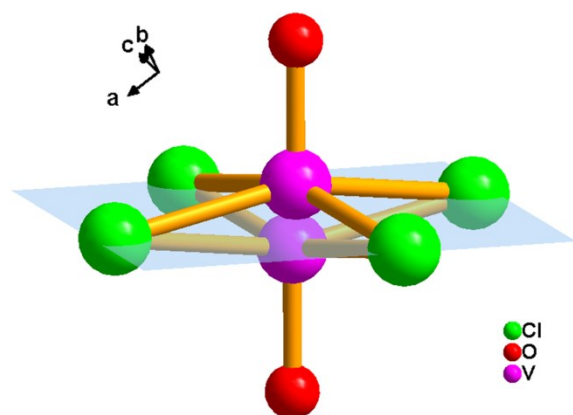


Fig. S2. The $[\text{VCl}_4\text{O}]^{2-}$ anions site disorder in **1**.

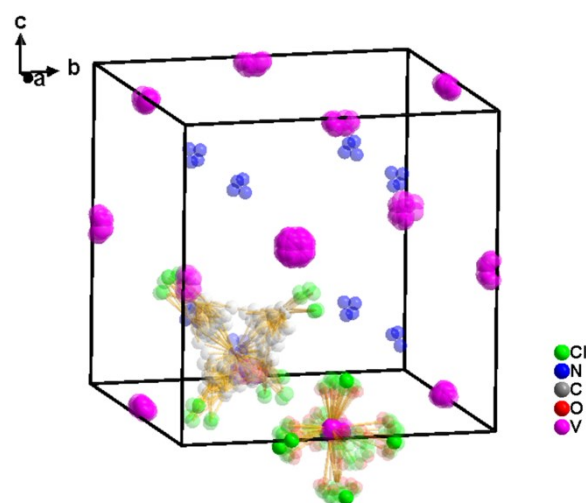


Fig. S3. The structure of **1** at 365 K. Hydrogen atoms, part of chlorine, oxygen, and carbon atoms were omitted for clarity.

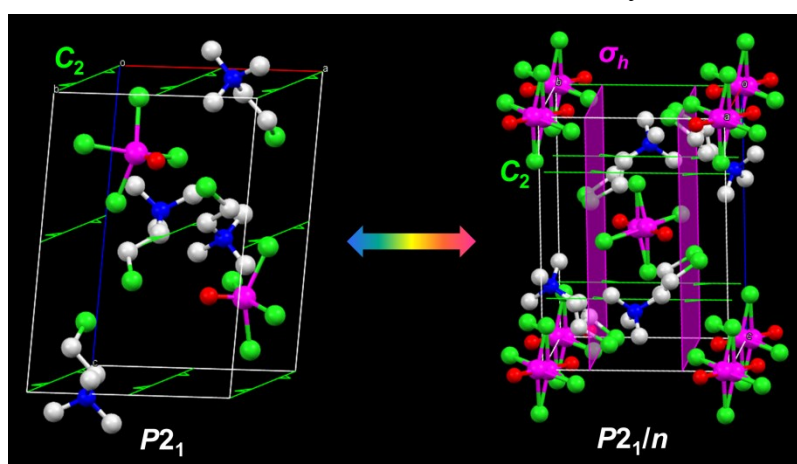


Fig. S4. Comparison of crystal structures at LTP and ITP for **1**.

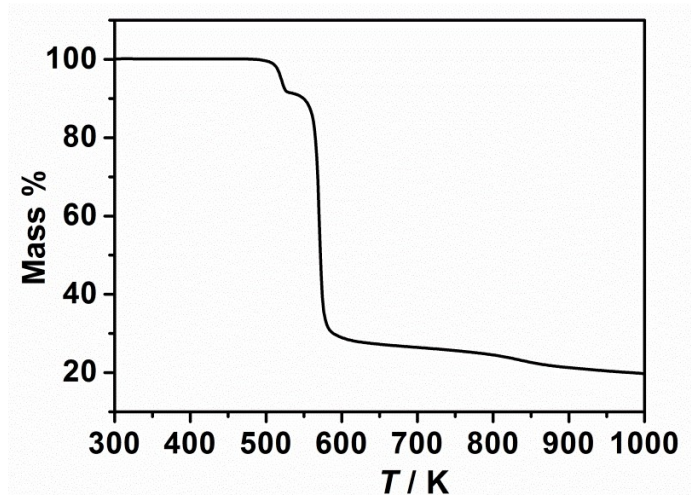


Fig. S5. TGA curve for 1.

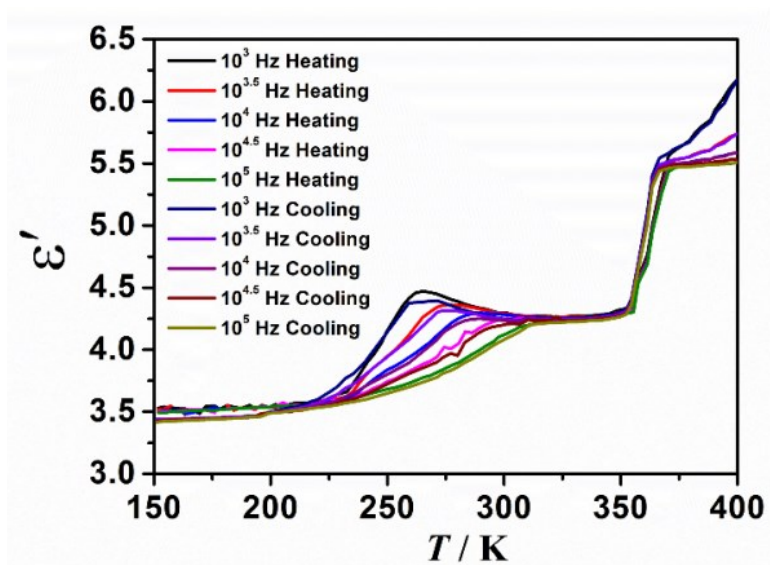


Fig. S6. Dielectric constant versus temperature at different frequencies with heating and cooling.

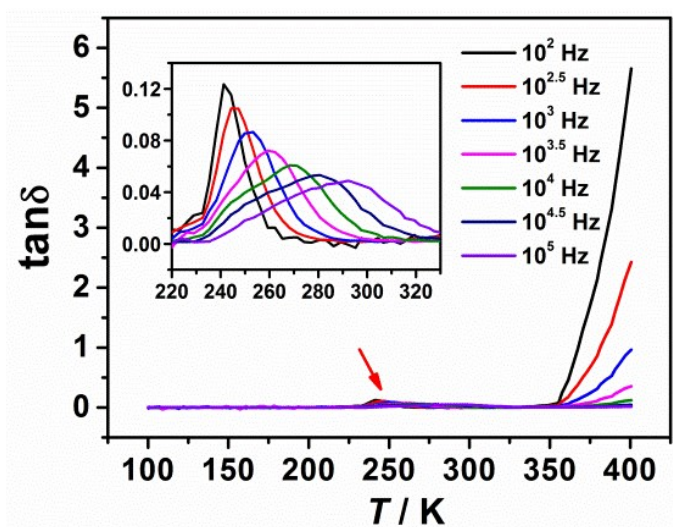


Fig. S7. The dielectric loss varied with frequencies and temperatures for 1.

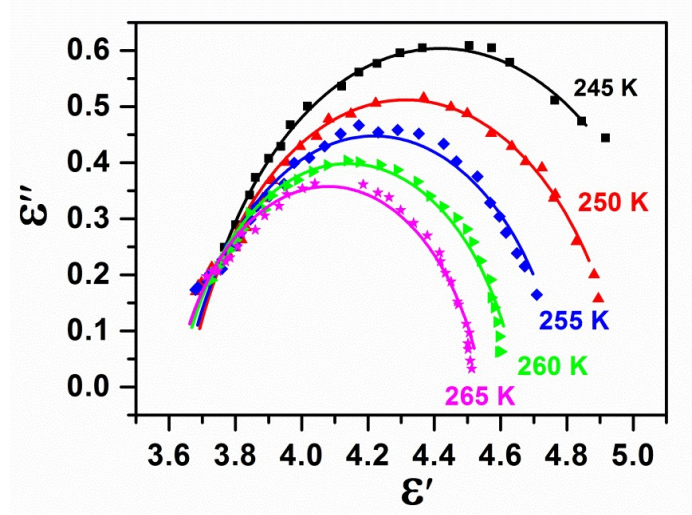


Fig. S8. Cole-Cole plot of **1** at temperatures 245 K, 250 K, 255 K, 260 K and 265 K.

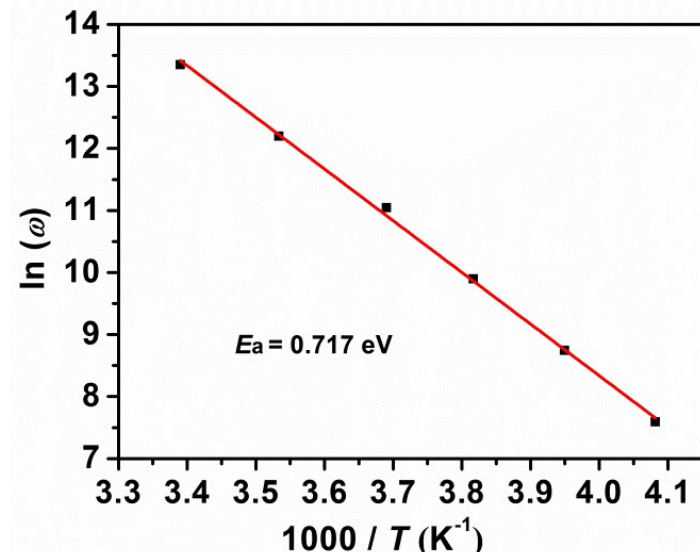


Fig. S9. Linear fitting of $\ln(\omega)$ versus $1000/T$ for **1**.

The activation energy for relaxation was estimated based on the Arrhenius equation from the plot of $1/T$ peak versus $\ln(\omega)$

$$\varepsilon''(T) = \frac{\omega\tau(T)}{1 + \omega^2\tau^2(T)} \quad \text{Eq. S1}$$

$$\frac{1}{\tau} = \omega_0 \exp\left(-\frac{E_a}{k_B T}\right) \quad \text{Eq. S2}$$

where f is the characteristic relaxation frequency, ω is angular frequency, $\tau(T)$ is the relaxation time, E_a is the activation energy for the phase transition, T_p is the temperature of an ε'' peak, and k_B is the Boltzmann constant, ω_0 is a pre-exponential factor.

Table S1. Fitting data of Cole-Cole semicircles of **1** at different temperatures.

T (K)	ε_0	ε_∞	τ (s)	α
245	5.17	3.66	6.12×10^{-4}	0.140
250	4.96	3.65	2.38×10^{-4}	0.157
255	4.79	3.64	1.20×10^{-4}	0.155
260	4.65	3.63	6.09×10^{-5}	0.156
265	4.54	3.62	3.27×10^{-5}	0.164

Table S2. Crystal data collection and structure refinement of **1** at different temperatures

Compound	$(C_5NClH_{13})_2VOCl_4$ (1)		
temperature (K)	200	300	365
phase	LTP	ITP	HTP
formula weight	453.97	453.97	453.97
crystal system	monoclinic	monoclinic	cubic
space group	$P2_1$	$P2_1/n$	$Fm\bar{3}m$
a (Å)	8.75140(10)	8.7533(4)	12.8565(11)
b (Å)	9.04080(10)	9.0953(4)	12.8565(11)
c (Å)	12.5409(2)	12.7626(6)	12.8565(11)
β (deg)	95.9650(10)	95.135(4)	90
volume (Å ³)	986.86(2)	1012.00(8)	2125.0(5)
Z	2	2	4
Scan mode	ω -scan	ω -scan	ω -scan
crystal size (mm ³)	$0.1 \times 0.2 \times 0.15$	$0.1 \times 0.2 \times 0.15$	$0.1 \times 0.2 \times 0.15$
μ (mm ⁻¹)	11.654	11.365	10.824
$F(000)$	466.0	466.0	932.0
radiation	Cu K α	Cu K α	Cu K α

2 θ range for data collection (deg)	7.088-151.23	11.784-148.122	11.922-125.092
index ranges	$-10 \leq h \leq 10$, $-11 \leq k \leq 11$, $-15 \leq l \leq 15$	$-7 \leq h \leq 10$, $-11 \leq k \leq 11$, $-15 \leq l \leq 15$	$-10 \leq h \leq 11$, $-13 \leq k \leq 10$, $-12 \leq l \leq 14$
density (calcd) (g cm ⁻³)	1.528	1.490	1.419
reflections collected	13844	10601	495
R_{int}	0.0476	0.0556	0.0338
Refinement method	full-matrix least-squares on F^2		
data/restraints/parameters	4026/1/188	2013/0/131	121/21/40
Goodness-of-fit on F^2	1.054	1.131	1.155
$R_1, \omega R_2$ [$I > 2\sigma(I)$]	0.0423, 0.1108	0.0758, 0.2182	0.0554, 0.1461
$R_1, \omega R_2$ [all data]	0.0444, 0.1124	0.0878, 0.2326	0.0918, 0.2003
$\rho_{\text{max}}, \rho_{\text{min}}$ (e \AA^{-3})	0.90, -0.43	1.08, -0.89	0.16, -0.19

References

- S1. G. Sheldrick, *Acta Crystallogr., Sect. A*, 2015, **71**, 3-8.
- S2. G. Sheldrick, *Acta Crystallogr., Sect. C*, 2015, **71**, 3-8.
- S3. O.V. Dolomanov, L.J. Bourhis, R.J. Gildea, J.A.K. Howard, H. Puschmann, *J. Appl. Crystallogr.*, 2009, **42**, 339-341.